Physicochemical Investigation of Nanostructures in Liquid Phases: Ytterbium Nitrate Ionic Clusters Confined in Ytterbium Bis(2-ethylhexyl) Sulfosuccinate Reversed Micelles and Liquid Crystals

Alessandro Longo,[†] Angela Ruggirello,[‡] and Vincenzo Turco Liveri*[,‡]

Department of Physical Chemistry, Università di Palermo, Viale delle Scienze Parco D'Orleans II, 90128 Palermo, Italy, and ISMN, Istituto per lo Studio dei Materiali Nanostrutturati, Via U. La Malfa 153, 90146 Palermo, Italy

Received June 8, 2006. Revised Manuscript Received October 30, 2006

The confinement of finite amounts of ytterbium nitrate in the nanoscopic space of ytterbium bis(2-ethylhexyl)sulfosuccinate ($Yb(DEHSS)_3$) reversed micelles dispersed in *n*-heptane has been investigated by UV−vis−NIR, FT-IR, and SAXS. The analysis of the experimental data is consistent with the hypothesis that $Yb(NO_3)_3$ is distributed among reversed micelles as small size ionic clusters surrounded by the Yb^{3+} surfactant counterions and anionic heads while the surfactant alkyl chains point toward the solvent medium. As a consequence of confinement and interfacial effects, the ionic clusters display photophysical properties different from those in the bulk state or isolated species. Moreover, the entrapment of $Yb(NO_3)_3$ involves some changes in the structural properties of reversed micelles attributable to the increase of the volume fraction of the hydrophilic matter confined in the micellar core. Preliminary WAXS experiments on $Yb(NO_3)_3/Yb(DEHSS)_3$ composites obtained by complete evaporation of volatile components (water and organic solvent) of the liquid $Yb(NO_3)_3$,water/$Yb(DEHSS)_3$/*n*-heptane samples showed that also in these systems $Yb(NO_3)_3$ is dispersed in the hydrophilic domains of the surfactant matrix as very small clusters.

Introduction

Sodium bis(2-ethylhexyl) sulfosuccinate (NaDEHSS) is a well-known surfactant widely employed to form in apolar media reversed micelles, namely, dynamic molecular aggregates characterized by the coexistence of two spatially separated nanodomains: a micellar core constituted by the surfactant hydrophilic heads and a hydrophobic shell formed by its hydrocarbon tails.[1] What makes such aggregates potentially useful is the ability to incorporate in their interior finite amounts of many ionic, polar, and amphiphilic substances leading to the building up of very interesting supramolecular nanostructures in apolar liquid phases.[2−4] In particular, we have recently reported that $Yb(NO_3)_3$, up to a salt to surfactant molar ratio of 0.1, can be stably confined in the core of quite dry NaDEHSS reversed micelles forming small size ionic clusters with new and distinct physicochemical properties different from those found in bulk or aqueous solutions.[5]

Another peculiarity of NaDEHSS is that a class of very interesting surfactants able to form reversed micelles without the addition of cosolvent can be derived by simply replacing the sodium counterion with many other cations.[6−8] Then, by appropriate choice of the nature of the counterion, specific functionalities can be conferred to the resulting micellar aggregates such as enhanced luminescence of the solubilized species, synthesis and stabilization of nanoparticles, and confinement of counterion−ligand complexes.[1,9] However, while some investigations concerning the confinement of finite amounts of inorganic salts in NaDEHSS reversed micelles are reported in the literature, quite absent are studies focused on their segregation in aggregates of such NaDEHSS derivatives.[2,10,11] In particular, taking into account the steadily growing importance of lanthanide (Ln)-based surfactants,[12] it should be of interest to investigate the ability of Ln-$(DEHSS)_3$ reversed micelles and liquid crystals to stabilize ionic nanostructures in their hydrophilic interior.

* Corresponding author. Tel.: +39 091 6459844. Fax: +39 091 590015. E-mail: turco@unipa.it.
[†] ISMN.
[‡] Università di Palermo.

(1) Turco Liveri, V. *Nanosurface Chemistry*; Rosoff, M., Ed.; Dekker: New York, 2001.
(2) Giordano, C.; Longo, A.; Turco Liveri, V.; Venezia, A. M. *Colloid Polym. Sci.* **2003**, *281*, 229.
(3) Giordano, C.; Longo, A.; Ruggirello, A.; Turco Liveri, V.; Venezia, A. M. *Colloid Polym. Sci.* **2004**, *283*, 265.
(4) Calandra, P.; Longo, A.; Ruggirello, A.; Turco Liveri, V. *J. Phys. Chem. B* **2004**, *108*, 8260.
(5) Ceraulo, L.; Filizzola, F.; Longo, A.; Ruggirello, A.; Turco Liveri, V. *Colloid Polym. Sci.* **2006**, *00*, 000.
(6) Eastoe, J.; Towey, T. F.; Robinson, B. H.; Williams, J.; Heenan, R. H. *J. Phys. Chem.* **1993**, *97*, 1459.
(7) Eastoe, J.; Steyler, D. C.; Robinson, B. H.; Heenan, R. H.; North, A. N.; Dore, J. C. *J. Chem. Soc., Faraday Trans. I* **1994**, *90*, 2479.
(8) Arcoleo, V.; Goffredi, M.; Turco Liveri, V. *J. Colloid Interface Sci.* **1998**, *198*, 216.
(9) Mwalupindi, A. G.; Blyshak, L. A.; Ndou, T. T.; Warner, I. M. *Anal. Chem.* **1991**, *63*, 1326.
(10) Turco Liveri, V. *Curr. Top. Colloid Interface Sci.* **1999**, *3*, 65.
(11) Marcianò, V.; Minore, A.; Turco Liveri, V. *Colloid Polym. Sci.* **2000**, *278*, 250.
(12) Binnemans, K.; Gorlier-Walrand, C. *Chem. Rev.* **2002**, *102*, 2303.

10.1021/cm0613408 CCC: $37.00
Published on Web 02/08/2007

To extend our previous studies and with the aim to emphasize the effects of the surfactant counterion nature on the salt confinement and peculiar structural and photophysical properties, we have undertaken an investigation on the entrapment of finite amounts of $Yb(NO_3)_3$ in $Yb(DEHSS)_3$ reversed micelles dispersed in apolar solvent. Moreover, taking into account that lanthanide salt/surfactant composites are potentially useful for realizing devices of technologic interest,[12] a preliminary structural characterization of $Yb(NO_3)_3$/$Yb(DEHSS)_3$ composites obtained by complete evaporation of volatile components (water and organic solvent) of the liquid $Yb(NO_3)_3$,water/$Yb(DEHSS)_3$/*n*-heptane samples was also carried out by WAXS.

Experimental Section

Materials. Sodium bis(2-ethylhexyl) sulfosuccinate (NaDEHSS, Sigma 99%) was dried under vacuum for several days before use. Ytterbium(III) nitrate pentahydrate (Aldrich, 99.9%) and *n*-heptane (Aldrich, 99%, spectrophotometric grade) were used as received. $Yb(DEHSS)_3$ was prepared by mixing appropriate amounts of an aqueous solution of $Yb(NO_3)_3$ with a 10^{-2} M aqueous solution of NaDEHSS. After aging, the precipitate was filtered, washed several times, and dried under vacuum.[9]

Methods. $Yb(NO_3)_3$-containing $Yb(DEHSS)_3$/*n*-heptane systems at various salt to surfactant molar ratio R_S ($R_S = [Yb(NO_3)_3]/[Yb(DEHSS)_3]$) were prepared by adding the appropriate amount of $Yb(DEHSS)_3$/*n*-heptane solution, at fixed surfactant concentration ($[Yb(DEHSS)_3] = 0.066$ M), to a weighed quantity of salt. The amount of water in each sample, expressed as the molar ratio W ($W = [water]/[DEHSS^-]$), was checked by recording a NIR spectrum in the 1800−2200 nm range.[2] The solubility of $Yb(NO_3)_3$ in $Yb(DEHSS)_3$/*n*-heptane solution was determined by visual inspection of samples prepared at various R_S values and kept at constant temperature (25 °C).

UV−vis−NIR spectra were recorded in the wavelength range 200−2200 nm with a Perkin-Elmer (Lambda-900) spectrometer using Suprasil quartz cells with 1 or 10 mm optical path length.

FT-IR spectra were recorded in the wavelength range 900−4000 cm^{-1} by a Perkin-Elmer (Spectrum BX) spectrometer. All spectra were recorded with a spectral resolution of 0.5 cm^{-1}.

SAXS patterns have been recorded by a laboratory instrumentation consisting of a Philips PW 1830 X-ray generator providing Cu Kα, Ni-filtered ($\lambda = 1.5418$ Å) radiation with a Kratky small-angle camera in the "finite slit height" geometry equipped with step scanning motor and scintillation counter. Each scattering spectrum of freshly prepared samples was subtracted by the cell and solvent contributions. Best-fit analyses were performed by the CERN minimization program called MINUITS.

X-ray powder diffraction spectra of salt/surfactant composites were performed by a Philips diffractometer (PW1050/39 X Change) equipped with a copper anode (Cu Kα, 1.5418 Å).

Results and Discussion

The solubilization of $Yb(NO_3)_3$ in $Yb(DEHSS)_3$/*n*-heptane solution is itself proof of its entrapment in the hydrophilic core of $Yb(DEHSS)_3$ reversed micelles because its solubility in pure *n*-heptane is practically zero. Instead, the thermodynamic solubility (i.e., in the presence of $Yb(NO_3)_3$ crystals) in 0.066 M $Yb(DEHSS)_3$/*n*-heptane solution at $W = 3$ ($W = [water]/[DEHSS^-]$), expressed as salt to surfactant molar ratio R_S ($R_S = [Yb(NO_3)_3]/[Yb(DEHSS)_3]$), was found to be $R_S = 0.69$ at 25 °C. Moreover, in the absence of salt crystals, supersaturated but quite stable samples (for at least 1 month) were also prepared up to a value of $R_S = 1.3$. This supersaturation effect, typical of nucleation processes in very small domains, emphasizes the role of the confinement in the nanosize hydrophilic core of reversed micelles which, owing to their peculiar structure, size, and dynamics, are able to influence significantly the nucleation process, leading to the inhibition of the crystal growth and precipitation of thermodynamic unstable samples.

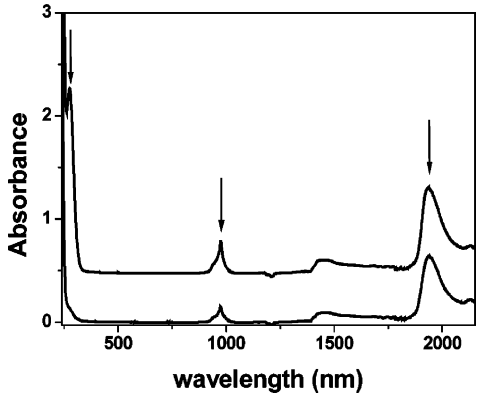

Figure 1. UV−vis−NIR spectra, subtracted by the solvent contribution, of $Yb(NO_3)_3$ containing water/$Yb(DEHSS)_3$/*n*-heptane ($W = 3.0$, $R_S = 0.69$, upper spectrum) and water/$Yb(DEHSS)_3$/*n*-heptane ($W = 2.3$, lower spectrum) systems at fixed surfactant concentration (0.066 M).

To gain photophysical and structural information on the state of $Yb(NO_3)_3$ ionic clusters confined in $Yb(DEHSS)_3$ reversed micelles, a UV−vis−NIR, FT-IR, and SAXS investigation as a function of R_S at fixed surfactant concentration ($[Yb(DEHSS)_3] = 0.066$ M) has been carried out. Moreover, when the theoretical and technological importance of inorganic salt/surfactant nanocomposites has been taken into account, some preliminary structural information on these systems, obtained by evaporation of the volatile components of the liquid samples, have also been achieved.[3]

UV−Vis-NIR Spectra. A typical UV−vis−NIR spectrum of $Yb(NO_3)_3$-containing water/$Yb(DEHSS)_3$/*n*-heptane system ($[Yb(DEHSS)_3] = 0.066$ M, $W = 3.0$, $R_S = 0.69$), subtracted by the solvent contribution and found in the 200−2200 nm wavelength range, is shown in Figure 1. For comparison, the subtracted spectrum of water/$Yb(DEHSS)_3$/*n*-heptane at the same surfactant concentration and $W = 2.3$ is also reported.

It must be noted that bands occur at about 300 nm owing to the symmetry-forbidden $n \rightarrow \pi^*$ transition of the nitrate anion,[13,14] at about 970 nm arising from the electric-dipole-forbidden and magnetic-dipole-allowed intraconfigurational transition $^2F_{7/2} \rightarrow {}^2F_{5/2}$ of Yb^{3+} [15,16] and at about 1920 nm owing to a combination mode of stretching and bending vibrations of water.[17,18]

(13) Tomisic, V.; Simeon, V. *Phys. Chem. Chem. Phys.* **1999**, *1*, 299.
(14) Eastoe, J.; Stebbing, S.; Dalton, J.; Heenan, R. *Colloid Surf. A* **1996**, *119*, 123.
(15) Lei, G.; Anderson, E.; Buchwald, M. I.; Edwards, B. C.; Epstein, R. I. *Phys. Rev. B* **1998**, *57*, 7673.
(16) Di Bari, L.; Lelli, M.; Pintacuda, G.; Piscitelli, G.; Marchetti, F.; Salvadori, P. *J. Am. Chem. Soc.* **2003**, *125*, 5549.
(17) Bonner, O. D.; Choi, Y. S. *J. Phys. Chem.* **1974**, *78*, 1723.
(18) Onori, G.; Santucci, A. *J. Phys. Chem.* **1993**, *97*, 5430.

Table 1. Wavelength (λ_{max}) and Molar Extinction Coefficient (ϵ_{max}) at the Band Maximum of Nitrate and Yb(III) in Yb(NO)$_3$,water/Yb(DEHSS)$_3$/*n*-heptane, Yb(NO)$_3$,water/NaDEHSS/*n*-heptane, Yb(NO)$_3$,water, and Solid Yb(NO)$_3$·5H$_2$O Systems

R_S	W	$\lambda_{max,NO3}$ (nm)	$\epsilon_{max,NO3}$ (M^{-1} cm^{-1})	$\lambda_{max,Yb}$ (nm)	$\epsilon_{max,Yb}$ (M^{-1} cm^{-1})
		Yb(NO)$_3$,water/Yb(DEHSS)$_3$/*n*-heptane [Yb(DEHSS)$_3$] = 0.066 M			
0	1.6			976	2.85
0	2.3			975	2.29
0.30	1.9	275	15.4	976	3.11
0.61	2.2	275	14.8	976	3.10
0.69	3.0	276	12.2	976	2.98
1.3[a]	3.5	276	12.1	976	3.03
		Yb(NO)$_3$,water/NaDEHSS/*n*-heptane [NaDEHSS] = 0.066 M			
0.05[b]	2.7	296	7.5	974	2.49
		Yb(NO)$_3$,water [Yb(NO)$_3$] = 0.090 M			
		301	7.1	972	1.94
		Yb(NO)$_3$·5H$_2$O Solid			
		270		971	

[a] Thermodynamically unstable sample. [b] Reference 5.

The wavelength (λ_{max}) and the molar extinction coefficient (ϵ_{max}) at the band maximum of nitrate and Yb(III) of all the investigated samples are collected in Table 1.

The visual comparison of the nitrate band in Yb(NO$_3$)$_3$,-water/Yb(DEHSS)$_3$/*n*-heptane system with those in Yb(NO$_3$)$_3$,water/NaDEHSS/*n*-heptane and Yb(NO$_3$)$_3$/water systems is shown in Figure 2. It can be noted that marked changes of the band position and intensity with respect to those in water and NaDEHSS reversed micelles occur. These changes can be taken as a first clue that, in the highly concentrated and restricted environment of the Yb(DEHSS)$_3$ reversed micelle core, the NO_3^- are mainly engaged in ion association with Yb^{3+}. In fact, such interaction stabilizes the nitrate ion ground state, leading to a hypsochromic shift.[13]

Besides, an inspection of data of Table 1 reveals that when R_S is increased, no significant changes of $\lambda_{max,NO3}$ and $\epsilon_{max,NO3}$ in the Yb(NO$_3$)$_3$,water/Yb(DEHSS)$_3$/*n*-heptane systems occur, while some *W* dependence of $\epsilon_{max,NO3}$ is observed. This suggests that, in the explored dimensional range, the size variation of Yb(NO$_3$)$_3$ ionic clusters confined within Yb(DEHSS)$_3$ reversed micelles does not influence significantly the photophysical properties of nitrate ions whereas some minor effects can be attributed to the change in the amount of water entrapped in the micellar core.[5] On the other hand, as is shown in Figure 3, significant changes in the band shape and position of the nitrate ion confined in Yb(DEHSS)$_3$ reversed micelles with respect to that in bulk solid Yb(NO$_3$)$_3$·5H$_2$O occur. This emphasizes effects due to the specific structural organization of the ionic cluster confined within the micellar core as well as interfacial interactions.

The Yb(III) NIR band in Yb(NO$_3$)$_3$/water, Yb(NO$_3$)$_3$,water/NaDEHSS/*n*-heptane, water/Yb(DEHSS)$_3$/*n*-heptane, and Yb(NO$_3$)$_3$,water/Yb(DEHSS)$_3$/*n*-heptane systems is shown in Figure 4. This band is characterized by a main peak occurring at about 975 nm accompanied by a side band due to lower energy transitions originating from excited sublevels thermally populated of the fundamental $^2F_{7/2}$ state.[16]

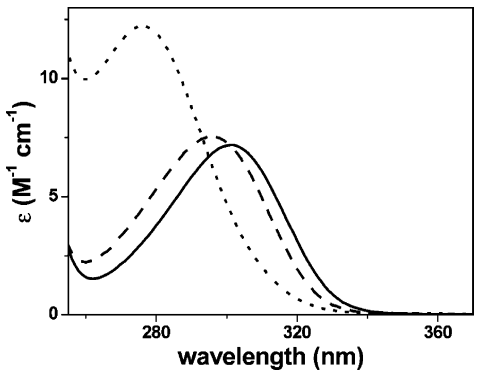

Figure 2. Nitrate UV band in Yb(NO$_3$)$_3$/H$_2$O (0.090 M, solid line) and Yb(NO$_3$)$_3$,water/NaDEHSS/*n*-heptane (W = 2.7, R_S = 0.05, dashed line) and Yb(NO$_3$)$_3$,water/Yb(DEHSS)$_3$/*n*-heptane (W = 3.0, R_S = 0.69, dotted line) systems at fixed surfactant concentration (0.066 M).

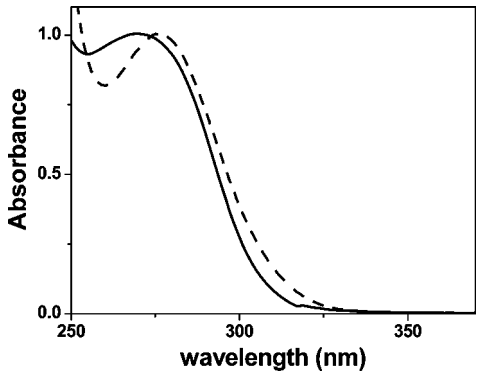

Figure 3. Comparison between the nitrate band, normalized at the same height of the band maximum, of Yb(NO$_3$)$_3$,water/Yb(DEHSS)$_3$/*n*-heptane ([Yb(DEHSS)$_3$] = 0.066 M, W = 3.0, R_S = 0.69, dashed line) system and Yb(NO$_3$)$_3$·5H$_2$O bulk solid (continuous line).

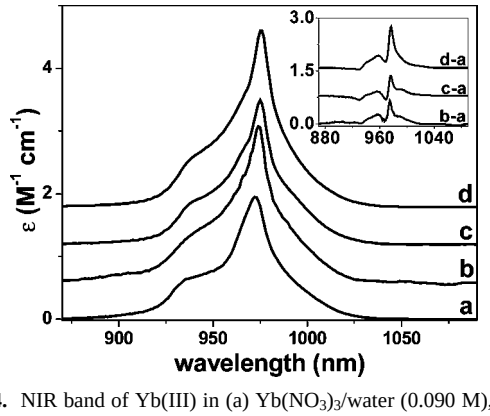

Figure 4. NIR band of Yb(III) in (a) Yb(NO$_3$)$_3$/water (0.090 M), (b) Yb(NO$_3$)$_3$,water/NaDEHSS/*n*-heptane (W = 2.7, R_S = 0.05), (c) water/Yb(DEHSS)$_3$/*n*-heptane (W = 2.3), and (d) Yb(NO$_3$)$_3$,water/Yb(DEHSS)$_3$/*n*-heptane (W = 3.0, R_S = 0.69) systems at fixed surfactant concentration (0.066 M).

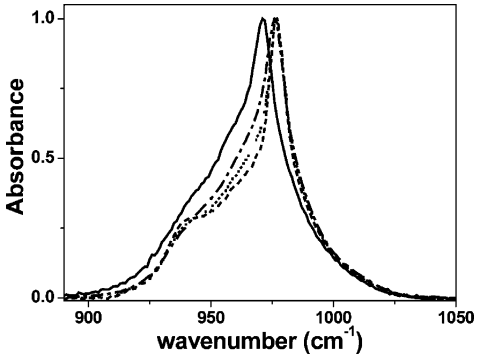

Figure 5. Normalized bands of Yb(III) confined in the micellar core (dashed line: $R_S = 0.30$; dotted line: $R_S = 0.61$; dash-dotted line: R_S=1.3) and in $Yb(NO_3)_3 \cdot 5H_2O$ bulk solid (continuous line).

To emphasize the changes with respect to aqueous Yb(III), the difference spectra are shown in the insert. It can be noted that in all the micellar systems positive deviations with respect to the band in water occur, and an inspection of data of Table 1 reveals that these deviations are also coupled with a red shift of $\lambda_{max,Yb}$ and an increase of $\epsilon_{max,Yb}$. On the other hand, minor changes in $\lambda_{max,Yb}$ and $\epsilon_{max,Yb}$ of the $Yb(NO_3)_3$,water/Yb(DEHSS)$_3$/*n*-heptane systems are induced by R_S and W variations. This is because the lanthanides band due to f−f transitions does not depend much on the chemical environment of the ion.[19] Moreover, considering the typical structure of salt containing reversed micelles,[20] existence in the $Yb(NO_3)_3$,water/Yb(DEHSS)$_3$/*n*-heptane system of at least two Yb(III) species can be reasonably hypothesized: one residing within the ionic cluster confined in the micellar core and another one located at its surface and formed by the Yb^{3+} counterions directly interacting with the surfactant anionic heads. In accordance with this hypothesis, we have attempted to obtain the spectrum of Yb(III) confined in the core of Yb(DEHSS)$_3$ reversed micelles by the equation

$$\epsilon_\lambda = X\epsilon_{\lambda,\text{core}} + (1 - X)\epsilon_{\lambda,\text{shell}} \quad (1)$$

where $\epsilon_{\lambda,\text{core}}$ is the molar extinction coefficient of the Yb(III) ions confined in the hydrophilic micellar core at the wavelength λ, X ($X = R_S/(1 + R_S)$) its molar fraction, and $\epsilon_{\lambda,\text{shell}}$ the molar extinction coefficient of the Yb(III) counterions at the micellar surface. It must be pointed out that the validity of eq 1 is based on the following assumptions: (i) the Yb(III) band in the $Yb(NO_3)_3$,water/Yb(DEHSS)$_3$/*n*-heptane systems is a combination of those in water/Yb(DEHSS)$_3$/*n*-heptane solutions and in the internal core and (ii) the contribution of Yb(III) ions at the cluster surface is independent of the R_S value. To minimize effects due to the W value and to simulate the contribution of the Yb(III) at the cluster surface, we used in our calculations the Yb(III) band of the sample at $R_S = 0$ and $W = 2.3$. The resulting bands of Yb(III) in the ionic cluster at various R_S values, normalized at the same height of the band maximum, are shown in Figure 5. For comparison, the Yb(III) band in $Yb(NO_3)_3 \cdot 5H_2O$ bulk solid is also shown. It can be noted that some changes in the band position and shape with respect to pure solid occur. These changes, as well as those induced by the R_S variation, confirm the occurrence of effects due to the specific structural organization of the ionic clusters within the micellar core and interfacial interactions.

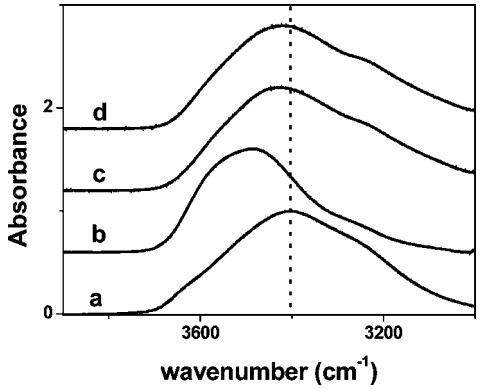

Figure 6. Water OH stretching band of (a) pure H_2O and (b) water/NaDEHSS/*n*-heptane ($W = 2.7$); (c) water/Yb(DEHSS)$_3$/*n*-heptane ($W = 2.3$); (d) $Yb(NO_3)_3$,water/Yb(DEHSS)$_3$/*n*-heptane ($W = 3.0$, $R_S = 0.69$) systems at fixed surfactant concentration (0.066 M).

FT-IR Spectra. IR spectroscopy was chosen as a suitable technique to investigate the $Yb(NO_3)_3$,water/Yb(DEHSS)$_3$/*n*-heptane system because on a time scale of about 10^{-13} s (shorter than most exchange processes occurring in the liquid phase) it allows simultaneous achievement of detailed information on the state and environment of several molecular groups of interest through an analysis of their band shape and position.[21] The most significant, which will be analyzed here, are the bands due to water OH (3000−3700 cm^{-1}), surfactant CO (1739 cm^{-1}), SO_3^- (1050 cm^{-1}), and salt NO_3^- (1250−1550 cm^{-1}) groups.

The water OH stretching bands in pure H_2O, water/NaDEHSS/*n*-heptane ($W = 2.7$), water/Yb(DEHSS)$_3$/*n*-heptane ($W = 2.3$), and $Yb(NO_3)_3$,water/Yb(DEHSS)$_3$/*n*-heptane ($W = 3.0$, $R_S = 0.63$) at fixed surfactant concentration (0.066 M) are shown in Figure 6. It can be noted that the position and shape of the OH stretching band in water/Yb(DEHSS)$_3$/*n*-heptane and $Yb(NO_3)_3$,water/Yb(DEHSS)$_3$/*n*-heptane systems are quite similar, while some changes with respect to the water/NaDEHSS/*n*-heptane system and pure water are observed. In particular, it is worth noting the band shift at lower frequencies with respect to the water/NaDEHSS/*n*-heptane system and the increase of the contribution of the lower frequency components with respect to pure water. These effects consistently emphasize that water molecules are preferentially engaged in the coordination shell of the Yb^{3+} ions. On the other hand, the absence of significant differences between the water OH stretching band in water/Yb(DEHSS)$_3$/*n*-heptane and $Yb(NO_3)_3$,water/Yb(DEHSS)$_3$/*n*-heptane systems suggests that Yb^{3+} ions located in the center and at the surface of the hydrophilic core are able to perturb quite similarly the vibrational dynamics of coordinated water.

Concerning the asymmetric peak centered at 1739 cm^{-1} and assigned to the surfactant CO stretching of the samples

(19) Bunzli, J. C. G. *Acc. Chem. Res.* **2006**, *39*, 53.
(20) Calandra, P.; Longo, A.; Marcianò, V.; Turco Liveri, V. *J. Phys. Chem.* **2003**, *107*, 6724.
(21) Calvaruso, G.; Minore, A.; Turco Liveri, V. *J. Colloid Interface Sci.* **2001,** *243*, 227.

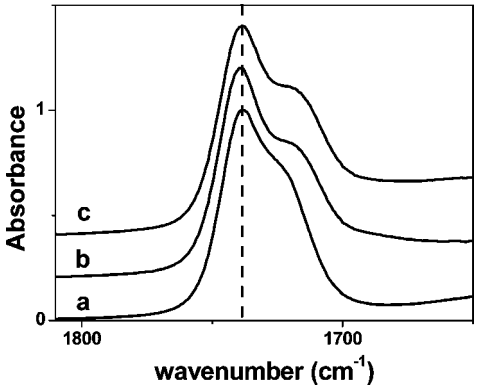

Figure 7. CO stretching band of (a) water/NaDEHSS/*n*-heptane ($W = 2.7$); (b) water/Yb(DEHSS)$_3$/*n*-heptane ($W = 2.3$); and (c) Yb(NO$_3$)$_3$,water/Yb(DEHSS)$_3$/*n*-heptane ($W = 3.0$, $R_S = 0.69$) systems at fixed surfactant concentration (0.066 M).

shown in Figure 7, it can be noted that the CO bands of the water/Yb(DEHSS)$_3$/*n*-heptane and Yb(NO$_3$)$_3$,water/Yb(DEHSS)$_3$/*n*-heptane systems are quite similar, while they are broader than that of the water/NaDEHSS/*n*-heptane system. Taking into account that no band shift is observed and a band broadening can be attributed to an enlargement of the spectrum of the surfactant head group conformations, it can be reasonably hypothesized that the CO groups are mainly located at the periphery of the hydrophilic core and they do not directly interact with the surfactant counterion even if their dynamics within the reversed micelle is influenced. In fact, this can be expected if one considers that the substitution of the single charged Na^+ with the triple charged Yb^{3+} should involve significant changes in the packing and dynamics of the surfactant molecules within each reversed micelle.

Concerning the band occurring in the 1250−1550 cm^{-1} range and assigned to the antisymmetric stretching of nitrate ions, it must be noted that it is sensitive to the nature of the surrounding species and, in the case of complex formation, to their binding orientation.[22] In particular, uncoordinated nitrate ions or forming solvent separated ion pairs are characterized by a broad band occurring in the range 1345−1400 cm^{-1},[23,24] whereas, in the case of complex formation with a rare earth ion, a typical monodentate nitrate band shows two peaks at about 1320 and 1450 cm^{-1} while a typical bidentate one shows them at about 1300 and 1500 cm^{-1}.[22]

The comparison of the antisymmetric stretching band of nitrate ions in Yb(NO$_3$)$_3$,water/Na(DEHSS)/*n*-heptane and Yb(NO$_3$)$_3$,water/Yb(DEHSS)$_3$/*n*-heptane systems at about the same water content is shown in Figure 8. It can be noted in the spectra of the Yb(NO$_3$)$_3$,water/Yb(DEHSS)$_3$/*n*-heptane systems two peaks at about 1290 and 1520 cm^{-1} which are practically absent in the Yb(NO$_3$)$_3$,water/Na(DEHSS)/*n*-heptane system. Then, according to the literature, this indicates that in the Yb(NO$_3$)$_3$,water/Yb(DEHSS)$_3$/*n*-heptane system the nitrate ions are engaged in complex formation with Yb^{3+} as bidentate ligands forming nanostructured clusters confined in the micellar cores.[5]

The effects on the surfactant SO_3^- stretching band arising from the counterion substitution or W and R_S changes are

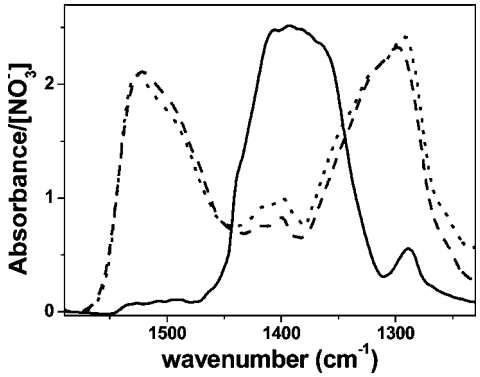

Figure 8. NO_3^- band of Yb(NO$_3$)$_3$,water/Na(DEHSS)/*n*-heptane ($W = 2.7$, $R_S = 0.05$, continuous line), Yb(NO$_3$)$_3$,water/Yb(DEHSS)$_3$/*n*-heptane ($W = 3.0$, $R_S = 0.69$; dotted line) and Yb(NO$_3$)$_3$,water/Yb(DEHSS)$_3$/*n*-heptane ($W = 3.5$, $R_S = 1.3$; dashed line) at fixed surfactant concentration (0.066 M).

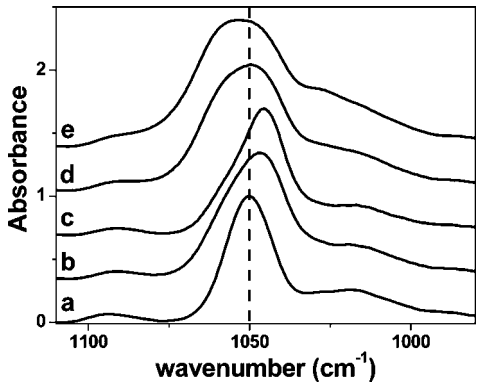

Figure 9. SO_3^- stretching band of (a) water/NaDEHSS/*n*-heptane ($W = 2.7$); (b) water/Yb(DEHSS)$_3$/*n*-heptane ($W = 2.3$); (c) water/Yb(DEHSS)$_3$/*n*-heptane ($W = 3.2$); (d) Yb(NO$_3$)$_3$,water/Yb(DEHSS)$_3$/*n*-heptane ($W = 3.0$, $R_S = 0.69$); (e) Yb(NO$_3$)$_3$,water/Yb(DEHSS)$_3$/*n*-heptane ($W = 3.5$, $R_S = 1.3$) systems at fixed surfactant concentration (0.066 M).

presented in Figure 9. It can be noted that the substitution of Na^+ with Yb^{3+} involves a red shift and an increase of the bandwidth. This finding clearly indicates that the SO_3^- groups, mainly located at the surface of the hydrophilic micellar core, are directly involved in interaction with the Na^+ or Yb^{3+} and their dynamics is significantly influenced by the counterion nature. Moreover, since the addition of the salt induces further position and shape changes, it can be argued that the entrapment of Yb(NO$_3$)$_3$ involves some structural and dynamical changes of the micellar core.

SAXS Spectra. Small-angle X-ray scattering data of samples at various R_S and W values and fixed surfactant concentration (0.068 M) are shown in Figure 10. All these SAXS spectra were well-described by a model of noninteracting polydisperse homogeneous scattering spheres. Since small-angle X-ray scattering is due to the contrast between regions with different electron densities and considering the reversed micelle structure, the scattering spheres of the model are to be interpreted as the bare or salt-containing hydrophilic micellar cores.[25,26]

The derived parameters, obtained following the fitting procedure previously described,[27] are the micellar core mean radius r_m and the parameter b, which is a quantitative

(22) Kanno, H.; Hiraishi, J. *J. Phys. Chem.* **1984**, *88*, 2787.
(23) Wahab, A.; Mahiuddin, S. *J. Chem. Eng. Data* **2004**, *49*, 126.
(24) Davis, R.; Irish, D. E. *Inorg. Chem.* **1968**, *7*, 1699.
(25) North, A. N.; Dore, J. C.; McDonald, J. A.; Robinson, B. H.; Heenan, R. K.; Howe, A. M. *Colloid Surf.* **1986**, *19*, 21.
(26) Mackeben, S.; Müller-Goymann, C. C. *Int. J. Pharm.* **2000**, *196*, 207.

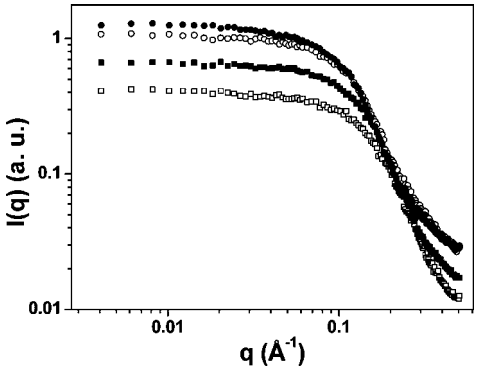

Figure 10. Smeared scattering profiles of $Yb(NO_3)_3$,water/$Yb(DEHSS)_3$/*n*-heptane system at various R_S and W values and fixed surfactant concentration (0.068 M). (□, $R_S = 0$, $W = 1.3$; ■, $R_S = 0.33$, $W = 1.8$; ○, $R_S = 0.69$, $W = 2.4$; ●, $R_S = 0.88$, $W = 2.8$).

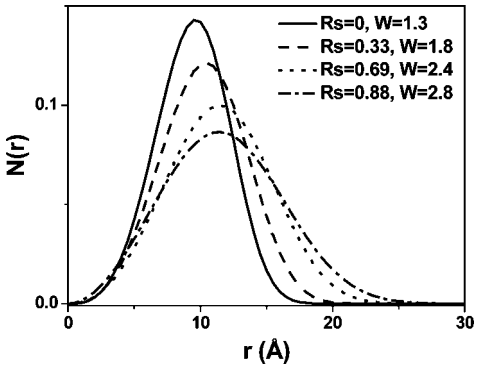

Figure 11. Size distribution function of the micellar core of bare and salt-containing $Yb(DEHSS)_3$ reversed micelles at various R_S and W values.

Table 2. Fitting Parameters Derived from SAXS Data as a Function of R_S and W at Fixed Surfactant Concentration ([$Yb(DEHSS)_3$] = 0.068 M)

R_S	W	r_m (Å)	b
0	1.3	9.4 ± 0.1	3.9 ± 0.1
0.33	1.8	10.3 ± 0.1	3.6 ± 0.1
0.69	2.4	11.5 ± 0.1	3.3 ± 0.1
0.88	2.8	11.8 ± 0.1	2.9 ± 0.1

descriptor of the size polydispersity. These parameters are collected in Table 2 and the size distribution functions of the hydrophilic core of bare and salt-containing $Yb(DEHSS)_3$ reversed micelles are shown in Figure 11.

A perusal of Table 2 and Figure 11 emphasizes that the increase of R_S and W causes a modest increase of the mean size of the micellar core accompanied by an enlargement of the size distribution involving the formation of bigger aggregates. These results suggest that the ionic clusters confined in the micellar cores are small and that the $Yb(NO_3)_3$ is quite inhomogeneously distributed among the reversed micelles. In particular, this last finding unveils the counteraction of the entropic tendency to salt dispersion among reversed micelles and the spontaneous unlimited growth of salt nuclei.

WAXS Spectra. Interesting salt/surfactant composites were obtained simply by evaporating under vacuum the solutions of salt-containing reversed micelles. Typical X-ray powder diffraction spectra of these $Yb(NO_3)_3/Yb(DEHSS)_3$ composites are compared to that of pure surfactant and salt

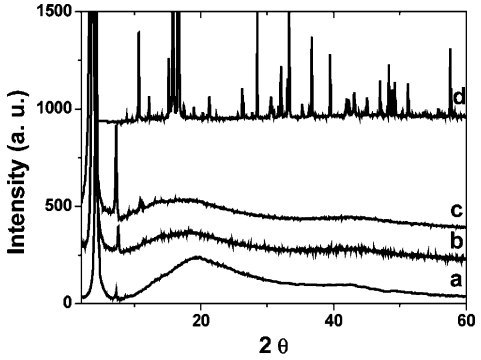

Figure 12. Comparison between the X-ray diffraction spectra of (a) pure $Yb(DEHSS)_3$, (b) $Yb(NO_3)_3/Yb(DEHSS)_3$ $R_S = 0.30$, (c) $Yb(NO_3)_3/Yb(DEHSS)_3$ $R_S = 0.59$, and (d) pure solid $Yb(NO_3)_3 \cdot 5H_2O$.

Table 3. Peak Position and Lattice Parameters of Pure and Salt Containing $Yb(DEHSS)_3$

R_S	2θ	d_{100} (Å)	2θ	d_{110} (Å)	2θ	d_{200} (Å)	2θ	d_{300} (Å)
0	4.25	20.8	7.25	12.2				
0.30	3.70	23.9			7.50	11.8	11.27	7.8
0.59	3.58	24.7			7.24	12.2	10.91	8.1

in Figure 12. The position of the peaks of pure $Yb(DEHSS)_3$ ($2\theta = 4.30$ and 7.30), converted in interplanar distances by the Bragg equation, were found to be in the ratio $1:1/\sqrt{3}$ (see Table 3). This involves that pure $Yb(DEHSS)_3$ is characterized by a two-dimensional hexagonal structure.[28]

On the other hand, the interplanar distances of the $Yb(NO_3)_3/Yb(DEHSS)_3$ composites were found to be in the ratio of 1:1/2:1/3, implying a one-dimensional lamellar structure. This change is also accompanied by a significant increase of the structural order emphasized by the marked increase of the peak intensity with R_S. Similar conclusion can be drawn by observing the broad peak at about $2\theta = 19°$ due to the amorphous domain formed by the surfactant tails which becomes less prominent when $Yb(NO_3)_3$ ionic clusters are entrapped inside the $Yb(DEHSS)_3$ matrix. It is also worth noting the absence in the spectra of $Yb(NO_3)_3/Yb(DEHSS)_3$ composites of the diffraction peaks of pure solid $Yb(NO_3)_3 \cdot 5H_2O$, assuring that the salt is dispersed in the surfactant liquid crystals in a quite disordered state. Moreover, a perusal of the lattice parameters of Table 3 indicates that by increasing R_S, a slight increase of the interplanar distance occurs, involving that $Yb(NO_3)_3$ is entrapped in the hydrophilic domains of the surfactant matrix as small size ionic clusters.

Conclusions

Through the analysis of UV−vis−NIR, FT-IR, and SAXS spectra, it has been proven that finite amounts of $Yb(NO_3)_3$ can be steadily confined within the hydrophilic core of $Yb(DEHSS)_3$ reversed micelles dispersed in *n*-heptane as small size ionic clusters composed of Yb^{3+}, NO_3^-, and water traces surrounded by the anionic surfactant head groups. A marked supersaturation effect leading to salt solubilization up to an unprecedented R_S value of 1.3 has been found. In the highly concentrated and restricted environment of the $Yb(DEHSS)_3$ reversed micelle core, water and NO_3^- ions are mainly

(27) Calandra, P.; Longo, A.; Turco Liveri, V. *J. Phys. Chem. B* **2003**, *107*, 25.

(28) Ekwall, P.; Mandell, L.; Fontell, K. *J. Colloid Interface Sci.* **1970**, *33*, 215.

engaged in association with Yb^{3+}, leading to a specific structural organization of the ionic clusters confined within the micellar cores. Both confinement and interfacial effects confer to these ionic clusters photophysical properties different from those in the bulk state or single species in aqueous solutions.

Finally, preliminary WAXS experiments on $Yb(NO_3)_3$/$Yb(DEHSS)_3$ composites, obtained by complete evaporation of volatile components (water and organic solvent) of the liquid $Yb(NO_3)_3$,water/$Yb(DEHSS)_3$/*n*-heptane samples, showed that also in these systems $Yb(NO_3)_3$ is dispersed in the hydrophilic domains of the surfactant matrix as quite disordered and very small ionic clusters.

Acknowledgment. The authors thank the University of Palermo (Università di Palermo, Fondi Ricerca Scientifica ex 60%) and MIUR (PRIN2004) for financial support.

CM0613408